

A new approach to extended focus for high-speed, high-resolution biological microscopy

Sara Abrahamsson^{*a}, Satoru Usawa^b and Mats Gustafsson^a

^aDepartment of Physiology, Program in Bioengineering, University of California San Francisco, 1700 – 4th Street, San Francisco, CA 94143-2532, USA

^bUniversity of California Berkeley, 16 Barker Hall, #3204, Berkeley, CA 94720-3204, USA

ABSTRACT

Microscopic study of rapid biological processes often requires both high resolution and high acquisition speed. When the speed requirement precludes acquiring a full 3D focal series at each time point, it can be attractive to sacrifice all axial information and instead record a single, 2D image per time point. This can be done at very high frame rates. High-resolution objectives, however, have a very short depth of focus. There are several established methods to achieve extended depth of focus, including annular pupil masks; mechanical sweeping of the focus and wavefront coding, which uses a pupil-plane optical device to introduce geometric aberrations. We have developed a new pupil plane approach where the light is manipulated chromatically rather than geometrically. A phase mask with circularly symmetric stair steps divides the pupil plane into a series of annular zones. The stair steps are large compared to the coherence length of the observation light, so that images from different zones form independently and combine incoherently into a final image. Each zone carries only a fraction of the objective's axial resolution, but the larger zones still carry the full lateral resolution of the objective. The incoherent addition of the different single-zone images results in a smooth and circularly symmetric point spread function with a depth of focus that is extended by a factor approximately equal to the number of zones in the mask. The method has been demonstrated both on bead samples and on whole cells with a performance that is well in accordance with the theoretical predictions.

Keywords: Extended focus, depth of field, high-speed imaging, wide-field microscopy, wavefront coding

1. INTRODUCTION

Most biological structures are inherently three-dimensional (3D), and are therefore best studied by 3D microscopy: by acquiring a focal series of 2D images from which a 3D reconstruction can be generated. Since the recording of a focus series involves multiple exposures and refocusing, requiring a significant amount of time, the repetition rate for time series imaging is limited. In the study of rapid biological processes this slow repetition rate can be a serious problem. If axial resolution is not crucial to the study in question, extended focus microscopy can be a good alternative, allowing for faster imaging since only one exposure per image is required. In extended focus microscopy the axial resolution is deliberately destroyed so that a 2D image with extended depth of focus is formed. In the case of wide-field microscopy, this extended-focus image is typically an approximation of the axial projection of a focus series. Since some amount of out-of-focus light is recorded together with the in-focus light, blur will be present in the image. This blurring can largely be removed by 2D deconvolution data processing, as long as the character of the blurring is approximately uniform through the depth of focus.

Several established extended focus schemes exist, based on either mechanical focus sweeping or optical manipulation of the focus. The mechanical method [1], [2] involves changing the objective-to-sample distance continuously during the exposure. An advantage of the mechanical sweeping approach is that the amount of focus extension is adjustable (the range over which the focus moves can be chosen freely by the operator for each data set). A drawback with the method, as it is currently implemented, is that the immersion fluid (which is necessary for high-resolution objectives) transmits

vibrations that can disturb a delicate sample. (In principle, this problem could be avoided by moving some downstream optical element instead of the sample or objective.) The mechanical motion required also limits the possible frame rate. The optical manipulation approach [3], [4], [5] has the advantage of allowing an extended focus image (albeit not deconvolved, see next section) to be viewed directly in the microscope eyepiece. The focus is extended by the insertion of some optical element in the beam path. This approach can be used both in wide-field and for scanning confocal microscopy. Wavefront Coding [6] is a wide-field microscopy method that uses a custom optical element near a pupil plane (the back focal plane of the objective, or an optically equivalent plane) to induce carefully chosen high-order geometric aberrations, extending the focus of the microscope to a degree determined by the optical element. An even simpler method involves an annular mask in the pupil plane [7]; this method has the severe drawback that most of the (often precious) observation light is discarded.

Here we describe a new type of pupil plane device that creates an extended focus by exploiting the finite coherence length of the observed light, rather than through geometric aberrations.

2. PRINCIPLE OF OPERATION

An extended focus can be defined as a uniform axial blurring at maintained lateral resolution. In other words, the point spread function (PSF) should be greatly elongated axially compared to a conventional high-resolution microscope, but not be significantly widened laterally. To allow 2D deconvolution to remove blurring, the lateral profile of the PSF should be approximately independent of axial position throughout the desired axial range. (The PSF describes how the system images a point source.)

The microscope resolution, both axial and lateral, is determined by the Numerical Aperture (NA) of the objective. The NA describes the cone angle over which the objective collects light and is defined by the back focal plane aperture of the objective. A high NA maximizes both axial and lateral resolution, as well as the amount of light collected. A lower NA would produce a lower axial resolution – that is, the desired longer depth of focus – but would sacrifice both lateral resolution and light collection efficiency. It is known [7] that an annular pupil-plane aperture produces a greatly extended focus at largely maintained lateral resolution (Fig. 1). A simple annular aperture (Fig. 1b) could thus be an excellent focus extension device, if it were not for the massive loss of light: only a small fraction of the available light is transmitted through the annulus. Light efficiency is a major concern in fluorescence microscopy in general and in time-lapse microscopy in particular. Photobleaching limits the length of the time series that can be recorded, and the exposure time of the individual extended-focus image ultimately sets the limit of the frame rate.

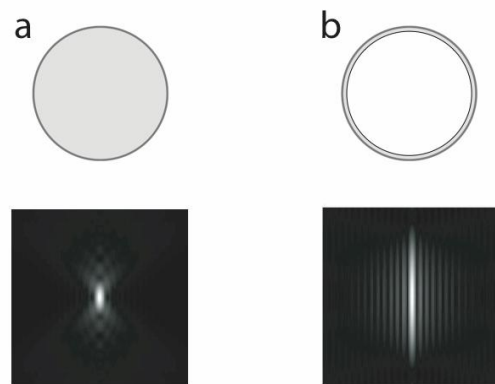


Fig. 1. Calculated PSFs for a full circular aperture (a), and a narrow annular aperture of the same outer diameter (b). The annular aperture produces the same lateral resolution as the full aperture, but only a small fraction of its axial resolution. This results in a PSF that is greatly extended axially, as desired for extended focus microscopy. However, the annular aperture discards most of the light from the sample, making the light efficiency too poor to be useful in fluorescence microscopy.

Our method modifies the annular-aperture idea in such a way that all of the light can be collected. If a typical microscope is divided into a series of concentric sub-apertures, each sub-aperture would produce a PSF with the desired extended depth of focus (Fig. 2b). In a normal microscope, light contribution from different annular zones adds coherently, producing the conventional PSF (Fig. 2a).

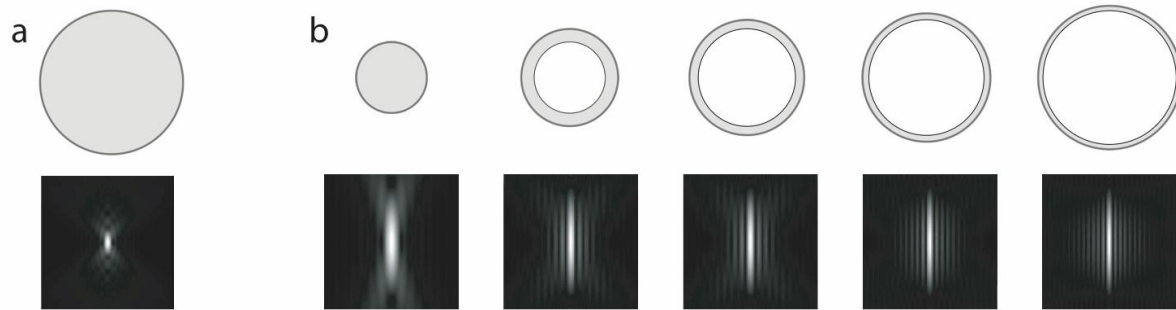


Fig. 2. Calculated PSFs for the full aperture (a) and each of a series of concentric sub-apertures (b). Each sub-aperture PSF is slightly different, but all are axially extended, corresponding to an increased depth of focus.

If the images formed by different annular sub-apertures could instead be added together incoherently (i.e., if all interference between different zones could be eliminated), they would form a combined PSF with the desired extended depth of focus (by a factor proportional to the number of apertures) while maintaining good axial resolution and light efficiency (Fig. 3).

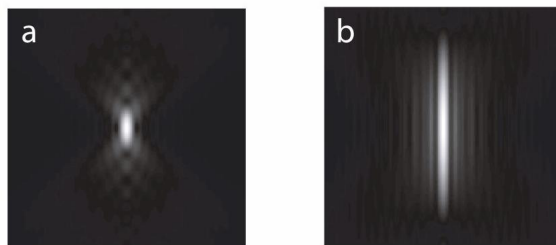


Fig. 3. The sum of the PSFs from the five sub-apertures in (b) has a dramatically extended focus, compared to the regular PSF (a), while retaining its narrow lateral width.

Our new method approximates this incoherent addition by phase-delaying the light from different sub-apertures by amounts that are large compared to the coherence length of the light. These phase delays (differences in optical path length) are introduced by a transmission mask shaped like a layer cake (Fig. 4). The device contains circularly symmetric stair steps that define the series of annular zones (the plateaus of the stair) corresponding to the sub-apertures in Fig. 2b. The stair steps induce an optical path length difference of $\delta l = h(n_m - 1)$ between adjacent plateaus, where h is the step height and n_m is the refractive index of the mask material. As long as δl is much longer than the coherence length of the observation light, the zones are rendered mutually incoherent and therefore act as separate apertures. Each sub-aperture produces an independent image, and the images formed add incoherently to form a final image in the manner described in Figs. 2 and 3. The mutual incoherence between different zones will of course not vanish completely for any finite step height, but an easily achievable step height of, say, 100 μm yields a very good approximation of the ideal, totally incoherent case.

3. MATERIALS AND METHODS

3.1 Manufacturing the stair step device

The main requirements for device performance is to ensure that each plateau is optically flat and that different plateaus are parallel to each other, and that the step height is sufficient. Photolithography would be an obvious manufacturing method, except that the step height (tens to hundreds of μm) is much larger than in typical lithography processes. We instead chose to assemble the device from separate disks. Our prototype stair step device was manufactured by LightMachinery, Inc. (Ottawa, Canada). A series of circular disks were cut from a single 200 μm thick etalon-grade fused silica substrate and optically contacted to each other and to an optically flat fused silica support (Spectra-Physics). Optical contacting was chosen since it ensures maximal parallelity - there is no cement involved that could cause a wedge angle between the discs. Wedge angles would cause the images from different zones to be laterally displaced relative to each other, which would decrease the lateral resolution performance. The combination of optical contacting with the excellent front-to-back parallelity of the etalon-grade substrate resulted in a parallelity better than $\lambda/20$ between all disks, as verified interferometrically on the finished device. Our prototype consists of four disks that each defines one sub-aperture. A fifth aperture is formed by the region between the outer edge of the largest disk and the edge of the (re-imaged) objective pupil. Alternative manufacturing methods could include molding the device from a preform, or high-precision diamond turning.

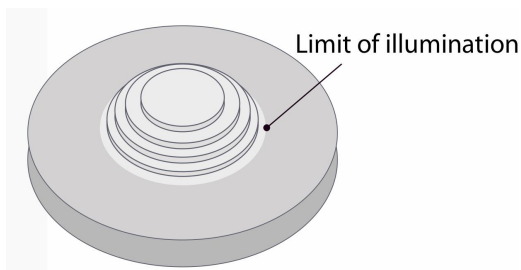


Fig. 4. Principle sketch of the stair step device. The stair steps divide the light into separate zones corresponding to the apertures of Fig. 2. The edge of the fifth zone is defined by the image of the microscope back-focal-plane aperture.

3.2 Simulations

The PSFs are calculated as the Fourier transform of the Pupil Function, multiplied by a defocus function, as described by Hanser *et al.* [9].

3.3 The microscope

Our extended focus scheme is incorporated into a home-built high-resolution wide field epifluorescence microscope. The stair step device is mounted in a removable, xyz-adjustable holder located in a secondary pupil plane of the microscope. (The primary pupil plane, i.e. back focal plane, of a high magnification objective is internal to the objective assembly and thus not accessible.)

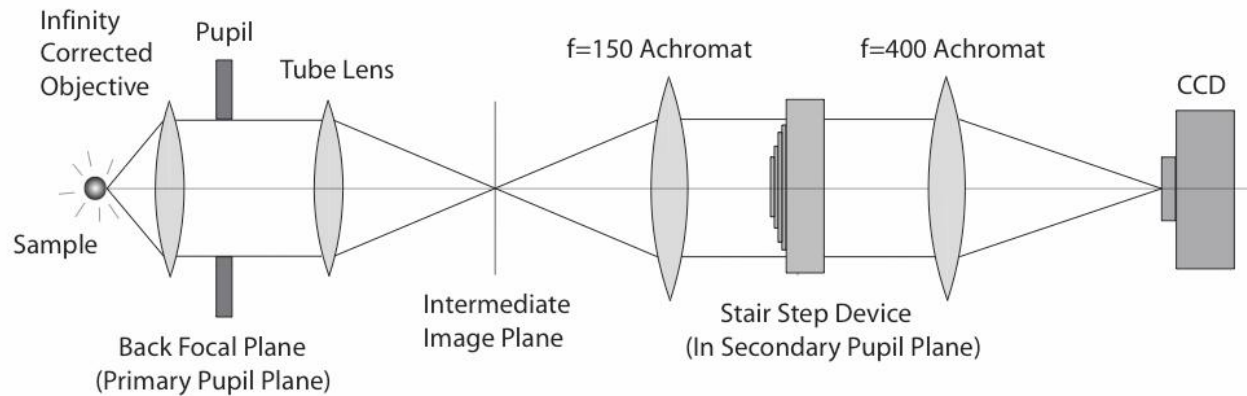


Fig. 5. Simplified diagram of the emission light path of the extended focus microscope setup.

Two different planapochromatic objective lenses were used for the imaging: a Leica water-immersion objective with an NA of 1.2 and a Leica oil-immersion objective with an NA of 1.4 and an internal aperture iris. The mask was designed to match the water objective, but the biological imaging was performed with the oil objective since it was less aberrated. (The aperture iris of the oil objective was stopped down to an NA of 1.2 in order for the beam size to fit to the diameter of the device in the pupil plane.) The microscope also contained a cooled, back-illuminated CCD camera (Ixon, Andor Technology, Belfast, Northern Ireland), a 500-550 nm bandpass emission filter (Chroma), and a Leica tube lens matched to the objectives.

3.4 Sample preparation

To evaluate the PSF of the imaging system, 100-nm-diameter fluorescent microspheres (yellow-green Fluospheres, Invitrogen Detection Technologies) were used. A drop of microspheres suspended in glycerol was placed on a cover slip and allowed to dry. The cover slip was then covered with a drop of water, placed on a microscope slide and sealed. The *Schizosaccharomyces pombe* strain YY105, expressing α -tubulin-GFP fusion protein, was cultured in YES medium and mounted for microscopy [10].

4. RESULTS

4.1 Point Spread Function measurements

The 3D PSF of the system, with and without the stair step device, was measured by imaging the 100 nm microspheres (Fig. 6). The depth of focus, as measured by the axial full width at half maximum (FWHM) of the PSF, was extended by a factor 4.7, from 0.74 μm to 3.5 μm whereas the lateral blurring (measured as lateral FWHM) increased only by a factor 1.2. The peak intensity decreased by about half due to the slight lateral blurring. These results are in good agreement with theoretical calculations (compare Fig. 3b). Larger amounts of focus extension can be achieved simply by increasing the number of disks.

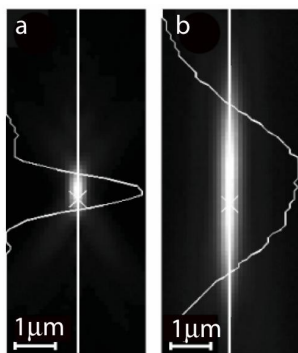


Fig. 6. Measured and experimental PSF in conventional and extended focus mode.

3.2 Live imaging

Microtubule movements in the fission yeast *Schizosaccharomyces pombe* expressing a fusion construct of GFP and α -tubulin. The cells of *S. pombe* are cylinders with a diameter of 3–4 μm and a length of 8–15 μm . In the interphase stage of the cell cycle, microtubules are present throughout most of the cell volume.

3.2.1 Conventional mode

To make a rough comparison for the performance of the stair step device, a focus series of a cell was taken in normal focus mode. The focus change between the sections was 0.2 μm so that the five images in Fig. 7a cover a focus of 1 μm . The exposure time was 0.1s per frame. Different microtubules, and different parts of each microtubule, are visible in each image within the focal series. To cover the full thickness of the cell without undersampling would require at least 10 images. In the sum of the images (Fig. 7b) all the tubules within the focus range can be seen at once. The extended focus scheme is used to create an approximation of this type of 2D extended focus image in a single exposure.

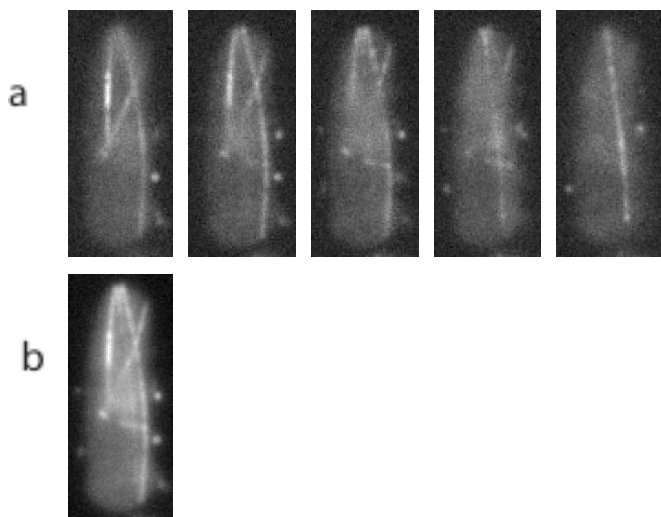


Fig. 7. Classical optical sectioning using a series of optical sections acquired at different focus positions (a). (The focus range shown here covers only part of the cell thickness). The sum of these optical sections (b) allows all the microtubules to be observed at once. Extended-focus microscopy optically produces an approximation of such a summed image series, and removes the associated blur through 2D deconvolution.

3.2.2 Microtubule movement

After installing the stair-step device in the microscope, a live *S. pombe* cell was observed 100 times over a period of 200 seconds, with an exposure time of 0.3s (longer than the normal exposure time because of the loss in peak intensity due to blurring). The focus extended throughout the thickness of the cell, and all the microtubules within the cell could be observed simultaneously (Fig. 8).

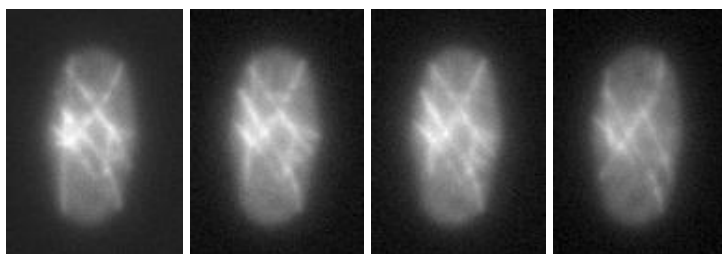


Fig 8. Extended focus images of an *S. pombe* cell. These images show the frames from $t = 0, 16, 18$ and 48 seconds. (These images are not deconvolved, but have been scaled individually to compensate for photobleaching.)

3.2.3. Computerized Deconvolution of Images

The lateral blurring produced by the extended focus can largely be removed by 2D image deconvolution, as long as the blurring characteristics are approximately the same throughout the depth of focus. The results of a simple Wiener filter on the *S. pombe* data is shown in Fig. 9. The image contrast is considerably improved compared to the raw data.

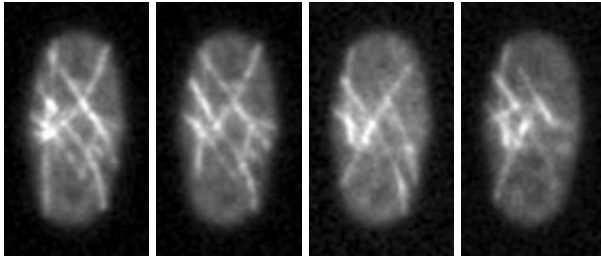


Fig 9. Wiener filtering, $t = 5, 17, 57, 86$ seconds

As an alternative deconvolution method, the same data were processed by the AIDA [8] algorithm (Fig. 10). Some noise amplification has occurred in the deconvolution. Details of the tubules, especially in areas with poor signal, can however be seen more clearly in the deconvolved data.

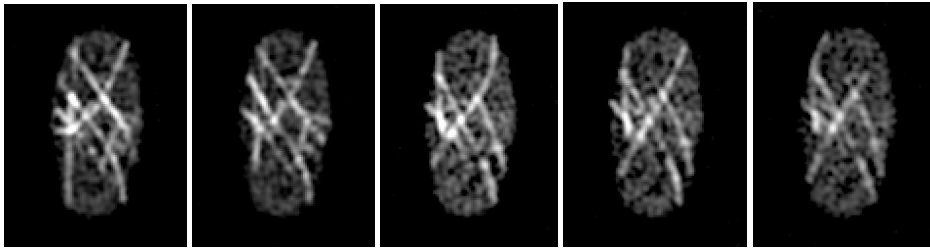


Fig 10. AIDA deconvolution. $t = 6, 17, 46, 54, 63$ seconds.

4. CONCLUSIONS

We have developed a new form of extended focus microscopy based on a circularly symmetric stair step device. The device extends the depth of focus by a factor approximately equal to the number of steps in the mask, without any loss of light. A prototype device extended the depth of field by a factor of 4.6, with a lateral blurring of only a factor of 1.2, which itself is largely removable by 2D deconvolution. This concept provides a new option for high-speed imaging of rapid biological processes.

5. ACKNOWLEDGEMENTS

We thank Satoru Uzawa for preparing the *pombe* cells and Göran Johansson, Lukman Winoto and Peter Kner for their part in building the microscope. This work was supported in part by the National Science Foundation through the Center for Biophotonics Science and Technology, by the Keck Laboratory for Advanced Microscopy, by the Sandler Family Supporting Foundation, and by the David and Lucille Packard Foundation.

REFERENCES

- [1] Häuser, 'A Method to Increase the Depth of Focus by Two Step Image Processing', *Optics Communications*, (vol 6, no 1, september 1972).
- [2] Juskaitis, Neil, Maussoumian, and Wilson, 'Strategies for Wide-Field Extended Focus Microscopy', *Focus on Microscopy 2001, Amsterdam*, conference presentation (2001).
- [3] Dowski and Cathey, 'Extended Depth of Field Through Wavefront Coding', *Applied Optics*, pp. 1859-1866 (vol 34, no 11, April, 1995).
- [4] Bradburn, Cathey, and Dowski, 'Realizations of Focus Invariance in Optical/Digital Systems with Wavefront Coding', *Applied Optics* (December 1997, vol. 36).
- [5] Juskaitis, Botcherby and Wilson, 'Scanning microscopy with extended depth of focus', *SPIE* (vol. 5701).
- [6] Cogswell, Chumachenko and Farrow, Oemagazine, 'Coming into Focus', *SPIE* (November 2003).
- [7] Min Gu, *Advanced Optical Imaging Theory*, 2000, Springer Verlag, ISBN 3540662626
- [8] Hom, Marchis, Lee, Haase, Agard, Sedat, 'AIDA; An Adaptive Image Deconvolution Algorithm with Application to Multi-Frame and Three-Dimensional Data' in preparation for submission to *J. Opt. Soc. Am.* (2005).
- [9] Hanser, Gustafsson, Agard, Sedat, 'Phase-retrieved pupil functions in wide-field fluorescence microscopy', *J Micr*, Vol. 216 October 2004, pp.32-48.
- [10] Sagolla, Uzawa and Cande. 'Individual microtubule dynamics contribute to the function of mitotic and cytoplasmic arrays in fission yeast', *J Cell Sci.* 2003 Dec 15;116(Pt 24)4891-930.